

Supplementary Information

High and temperature-insensitive ferroelectric remanent polarization in BiFeO₃-based Lead-free Perovskite

Min Zhang,^{a,d} Xiaoyan Zhang,^{a,b,c} Shyamashis Das,^{d,e} Zhiming M. Wang,^e Xiwei Qi,^{a,b,c*} Qiang Du^b

^aSchool of Materials Science and Engineering, Northeastern University, Shenyang 110819, China

^bSchool of Resources and Materials, Northeastern University at Qinhuangdao, Qinhuangdao 066004, China

^cKey Laboratory of Dielectric and Electrolyte Functional Materials Hebei Province, School of Resources and Materials, Northeastern University at Qinhuangdao, Qinhuangdao 066004, China

^dInstitut National de la Recherche Scientifique, 1650 Boulevard Lionel-Boulet, Varennes, J3X 1S2, Quebec, Canada

^eInstitute of Fundamental and Frontier Sciences, University of Electronic Science and Technology of China, Chengdu, 610054, China

Corresponding author: Xiwei Qi: E-mail: qxw@mail.neuq.edu.cn

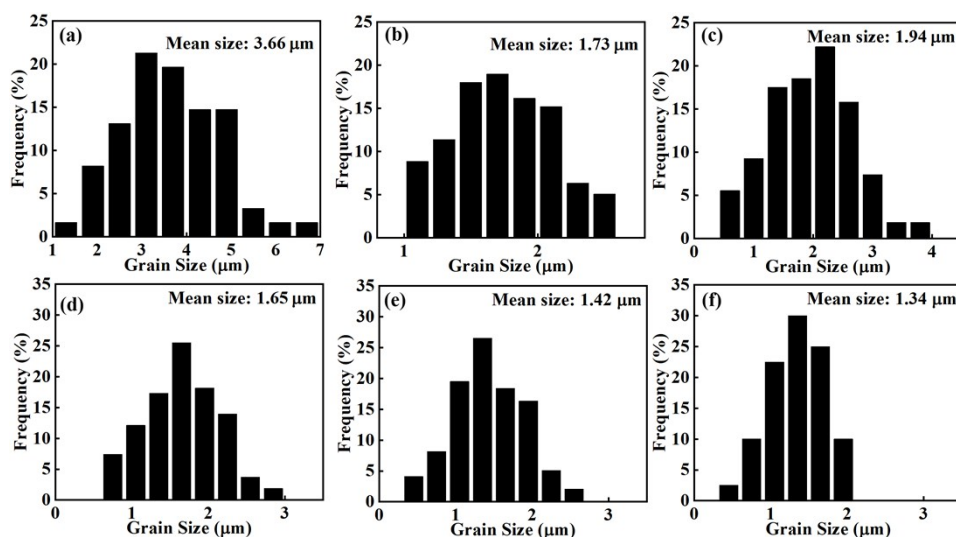


Fig. S1 Particle size distribution of BFO-BTO-LFO-Mn-x ceramics: (a) $x=0$, (b) $x=0.5$, (c) $x=1.0$, (d) $x=2.0$, (e) $x=3.0$ and (f) $x=4.0$.

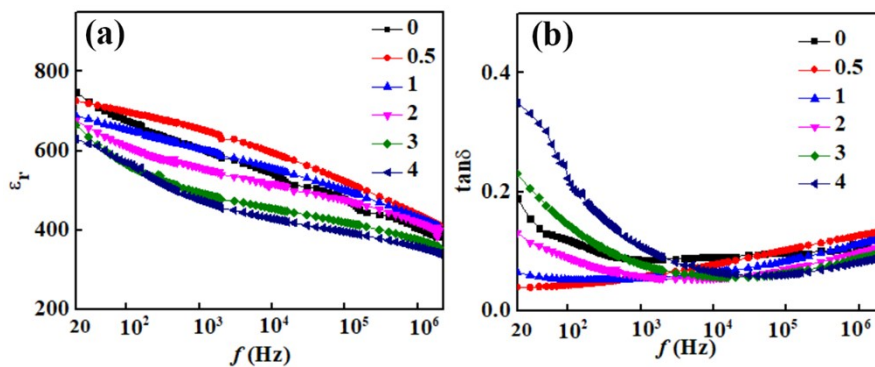


Fig. S2 (a) Relative dielectric constants ϵ_r and (b) dielectric losses $\tan\delta$ of BFO-BTO-LFO-Mn-x ($x=0-4.0$) ceramics.

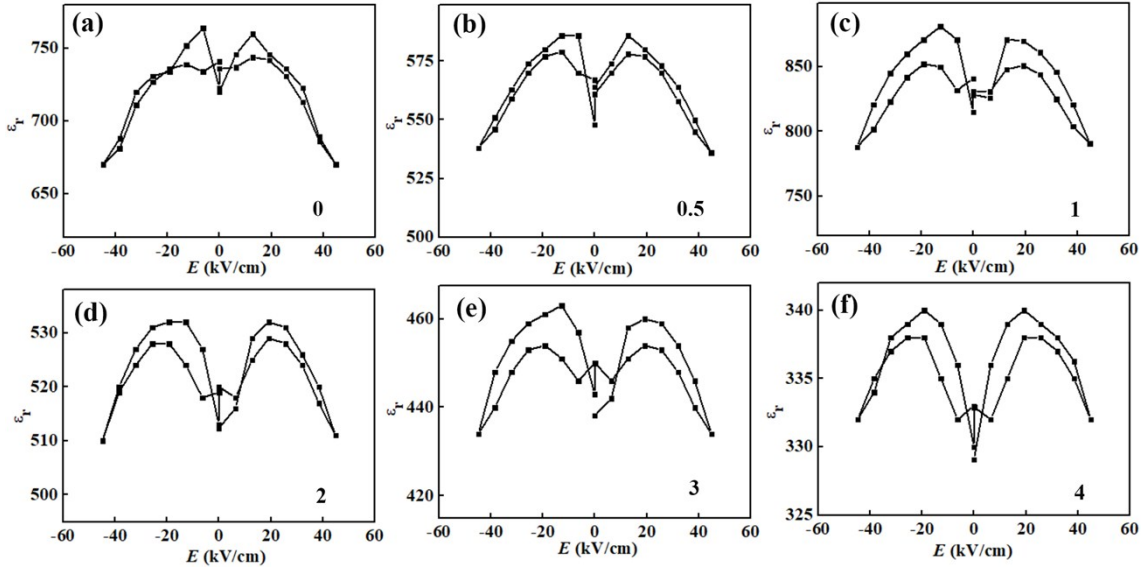


Fig. S3 Dielectric constant as a function of electric field of BFO–BTO–LFO–Mn– x ($x=0-4.0$) ceramics.

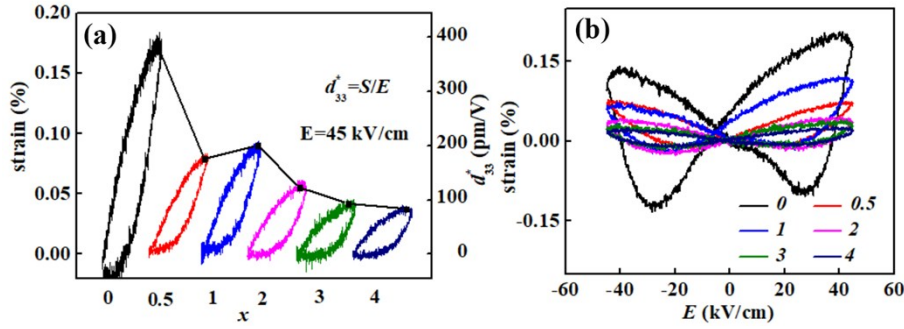


Fig. S4 Dielectric constant as a function of electric field of BFO–BTO–LFO–Mn– x ($x=0-4.0$) ceramics.

Fig. S4 shows the bipolar and unipolar strain curves of BFO–BTO–LFO–Mn– x measured at 1 Hz with an electric field of 45 kV/cm. Notably, the strains of undoped ceramics exceed those of doped ones. With the increasing of MnO_2 content, the S_{\max} firstly increases and then decreases, reaches its maximum value (about 0.09%) when $x=1.0$. The large signal d_{33}^* values are calculated by Eq. S(1):

$$d_{33}^* = \frac{S_{\max}}{E_{\max}} \quad \text{S(1)}$$

Where E_{\max} is 45 kV/cm and S_{\max} is the unipolar strain at 45 kV/cm. The d_{33}^* values of all the MnO_2 -doped samples firstly increase and then decrease as the MnO_2 content increases, and the value of d_{33}^* of $x=1.0$ sample is the highest (d_{33}^* : 200 pm/V).

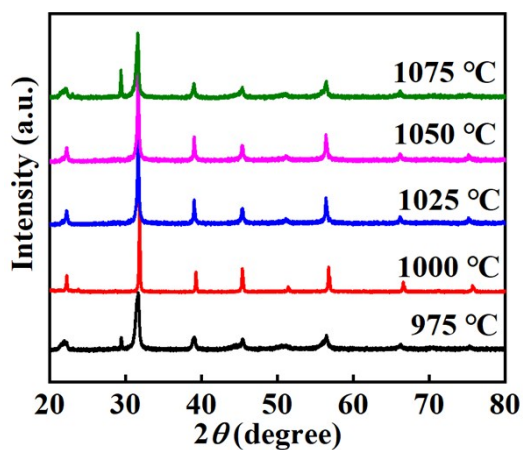


Fig. S5 XRD patterns of BFO-BTO-LFO-Mn-1 ceramics sintered at different temperature.

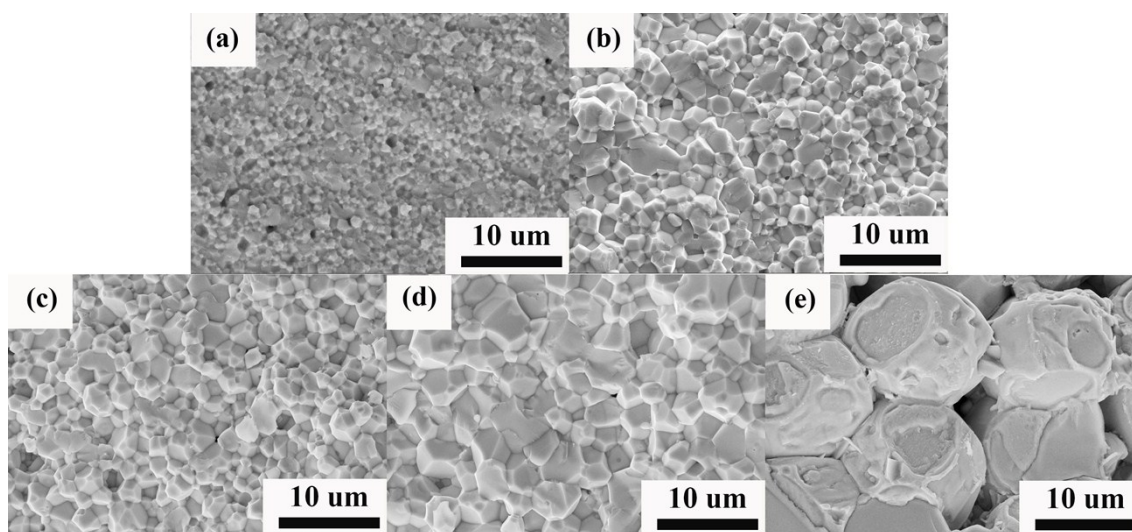


Fig. S6 SEM of BFO-BTO-LFO-Mn-1 ceramics sintered at (a) $T=975^{\circ}\text{C}$, (b) $T=1000^{\circ}\text{C}$, (c) $T=1025^{\circ}\text{C}$, (d) $T=1050^{\circ}\text{C}$, (e) $T=1075^{\circ}\text{C}$.

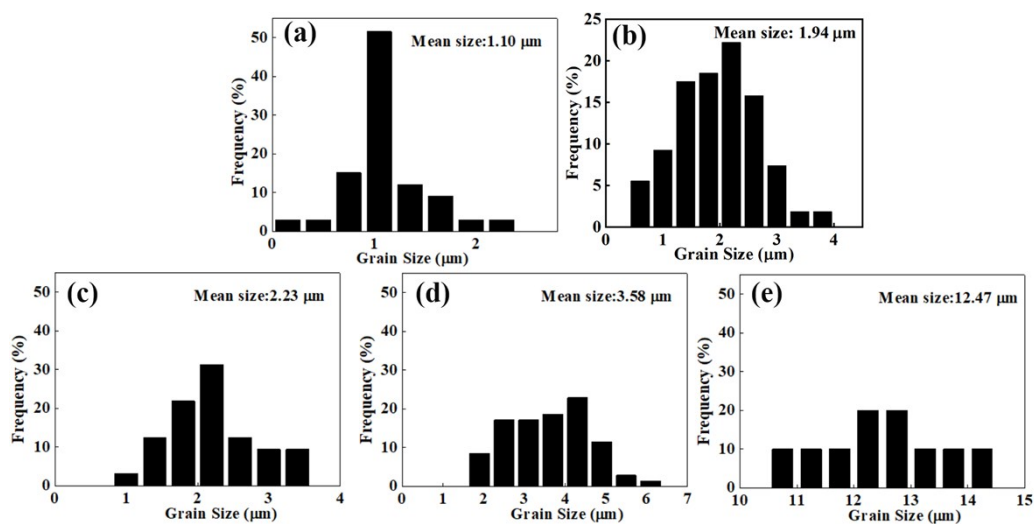


Fig. S7 Particle size distribution of BFO-BTO-LFO-Mn-1 ceramics: sintered at (a) $T=975^{\circ}\text{C}$, (b) $T=1000^{\circ}\text{C}$, (c) $T=1025^{\circ}\text{C}$, (d) $T=1050^{\circ}\text{C}$, (e) $T=1075^{\circ}\text{C}$.

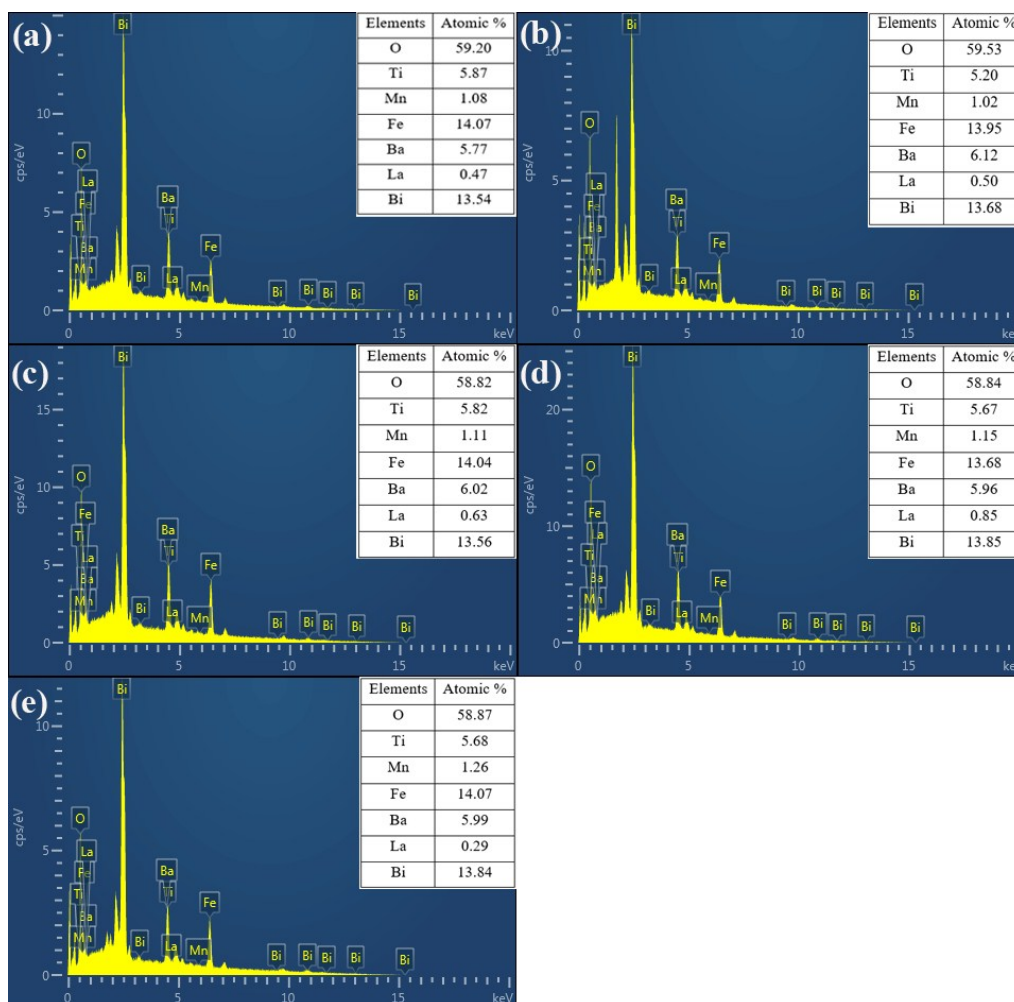


Fig. S8 EDS patterns of BFO–BTO–LFO–Mn–1 ceramics sintered at (a) T=975°C, (b) T=1000°C, (c) T=1025°C, (d) T=1050°C, (e) T=1075°C.

In order to confirm that the high temperatures of sintering the Bi volatility is inexistent, the EDS of BFO–BTO–LFO–Mn–1 ceramics sintered at different temperatures are shown in Fig. S8. The patterns describe that all the elements present in the BFO–BTO–LFO–Mn–1 samples. And these spectra further reveal that there are no extra elements present in all the samples. The mole percentages of the concentrations in each of the samples were estimated, and the obtained ratio of elements comes close to the empirical formula of BFO–BTO–LFO–Mn–1 system and thus confirms that the high temperatures of sintering the Bi volatility is inexistent.

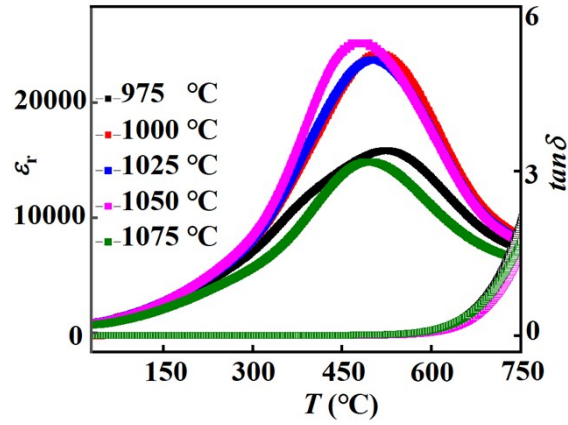


Fig. S9 Temperature-dependent dielectric properties of BFO-BTO-LFO-Mn-1 ceramics sintered at 975–1075 °C.

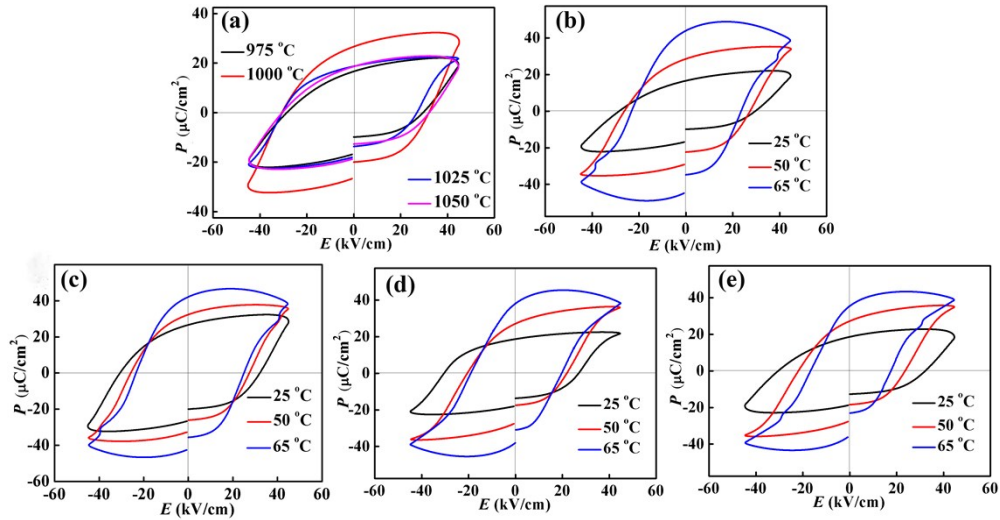


Fig. S10 P - E loops of BFO-BTO-LFO-Mn-0 ceramics (a) sintered at 975–1075 °C measure at room temperature and measure at different temperatures sintered at: (b) $T=975^{\circ}\text{C}$, (c) $T=1000^{\circ}\text{C}$, (d) $T=1025^{\circ}\text{C}$, (e) $T=1050^{\circ}\text{C}$.

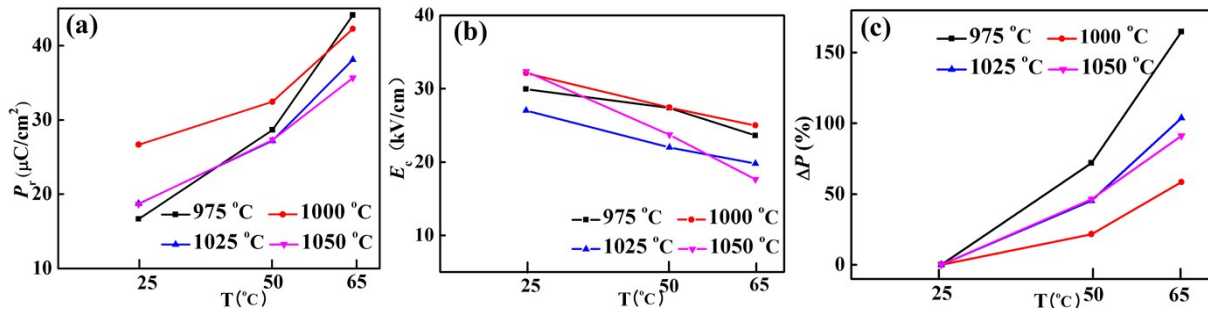


Fig. S11 (a) Remanent polarization P_r (b) coercive field E_c and (c) the P_r variation of BFO-BTO-LFO-Mn-0 ceramics at different measure temperatures.

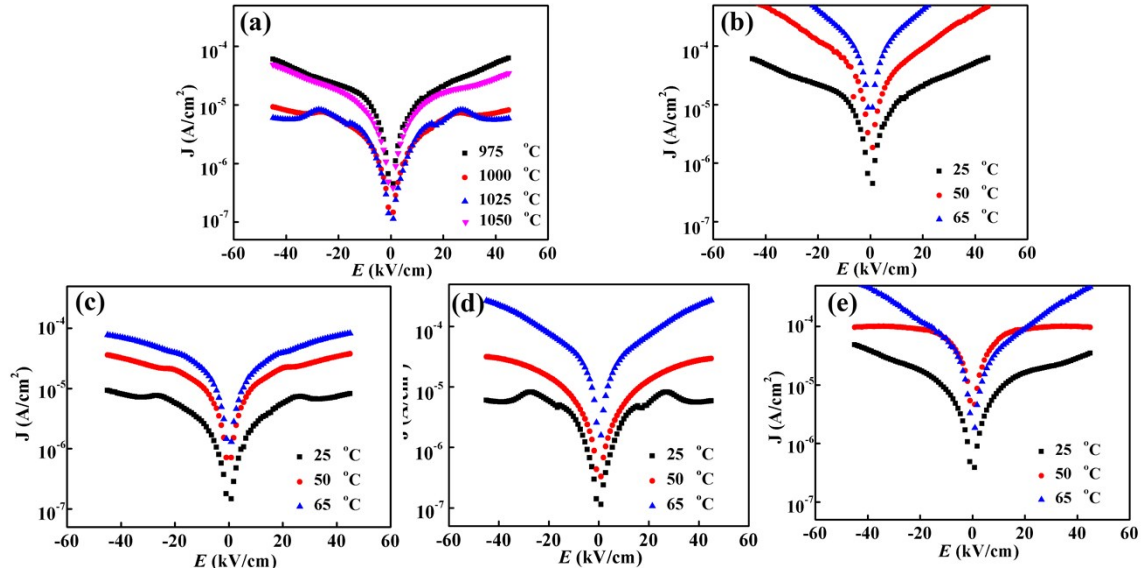


Fig. S12 Leakage current density of BFO–BTO–LFO–Mn–0 ceramics (a) sintered at 975–1075 °C measure at room temperature and measure at different temperatures sintered at: (b)T=975°C, (c) T=1000°C, (d) T=1025°C, (e) T=1050°C.

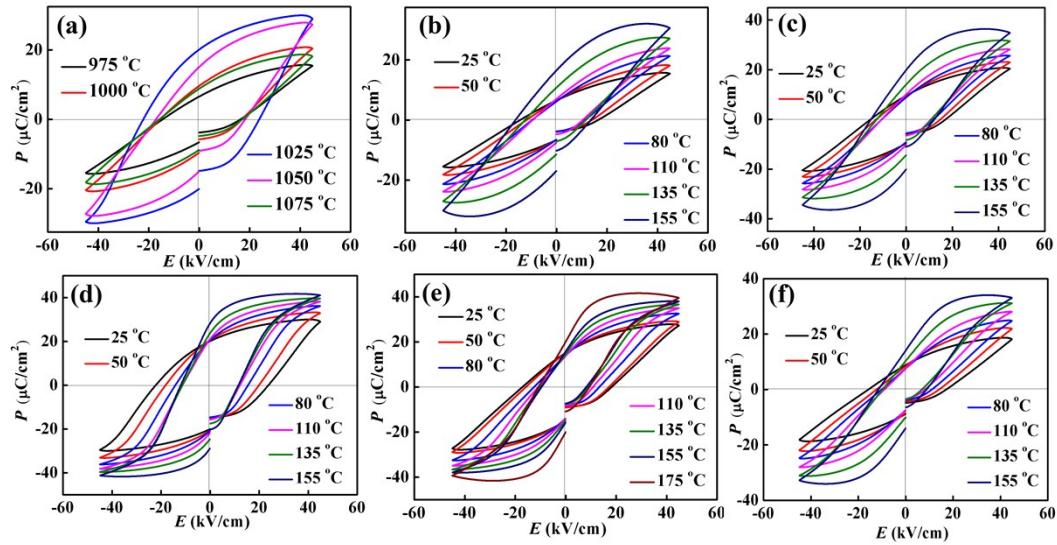


Fig. S13 P - E loops of BFO–BTO–LFO–Mn–0.5 ceramics (a) sintered at 975–1075 °C measure at room temperature and measure at different temperatures sintered at: (b)T=975°C, (c) T=1000°C, (d) T=1025°C, (e) T=1050°C, (f) T=1075°C.

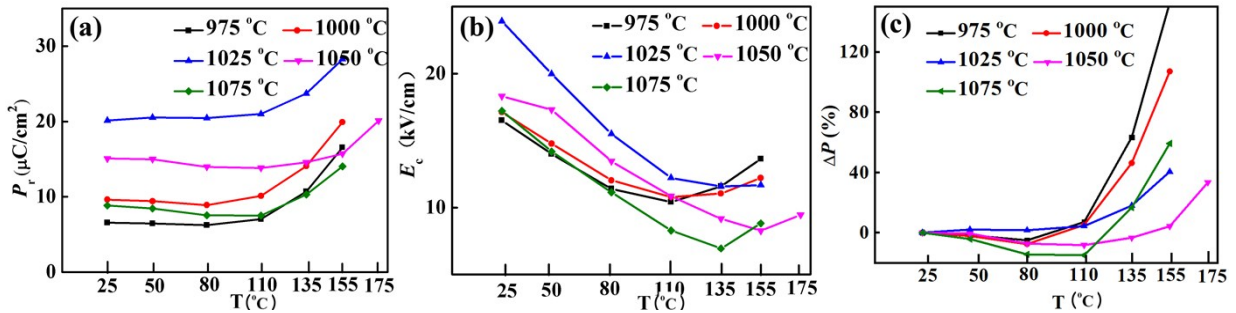


Fig. S14 (a) Remanent polarization P_r (b) coercive field E_c and (c) the P_r variation of BFO–BTO–LFO–Mn–0.5 ceramics at different measure temperature.

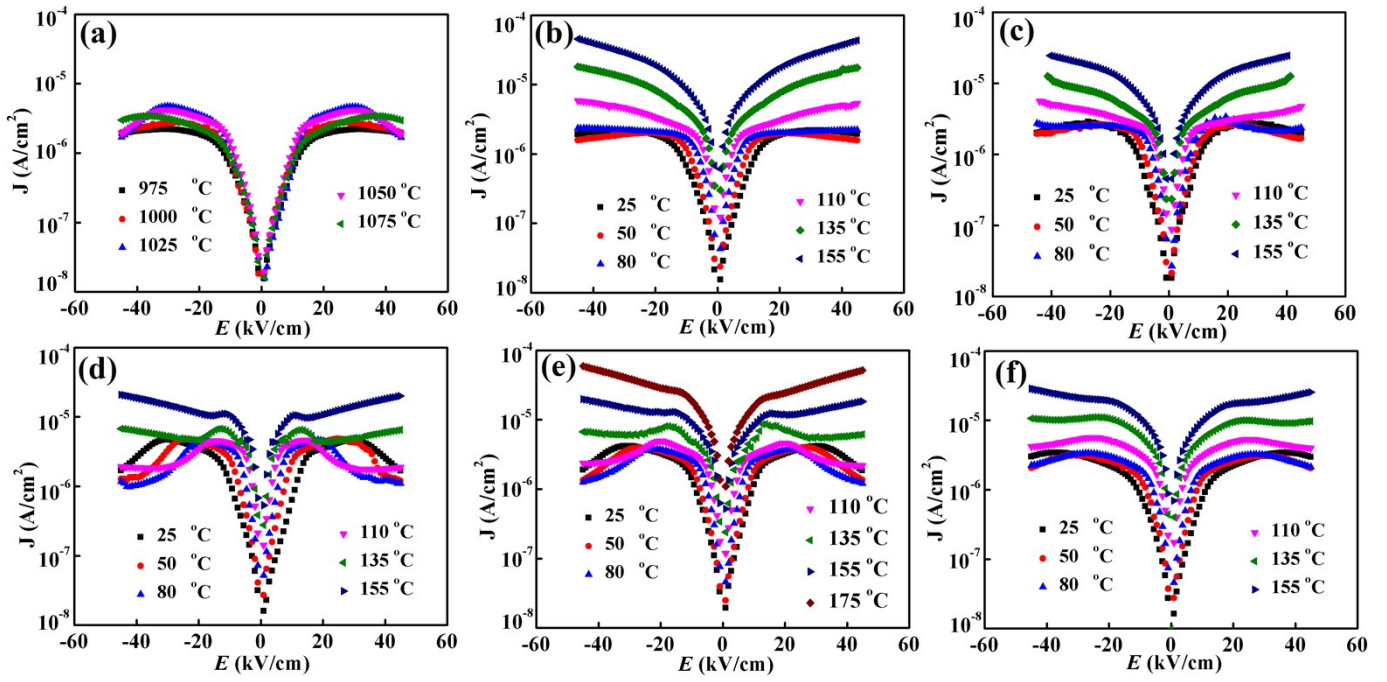


Fig. S15 Leakage current density of BFO-BTO-LFO-Mn-0.5 ceramics (a) sintered at 975–1075 °C measure at room temperature and measure at different temperatures sintered at: (b) T=975°C, (c) T=1000°C, (d) T=1025°C, (e) T=1050°C, (f) T=1075°C.